Bond Dissociation Energies and Radical Stabilization Energies Associated with Model Peptide-Backbone Radicals

Geoffrey P. F. Wood,[†] Damian Moran,[†] Rebecca Jacob,[‡,§] and Leo Radom*[,†,‡]

School of Chemistry, University of Sydney, Sydney, NSW 2006, Australia, and Research School of Chemistry, Australian National University, Canberra, ACT 0200, Australia

Received: April 11, 2005; In Final Form: May 17, 2005

Bond dissociation energies (BDEs) and radical stabilization energies (RSEs) have been calculated for a series of models that represent a glycine-containing peptide-backbone. High-level methods that have been used include W1, CBS-QB3, U-CBS-QB3, and G3X(MP2)-RAD. Simpler methods used include MP2, B3-LYP, BMK, and MPWB1K in association with the 6-311+G(3df,2p) basis set. We find that the high-level methods produce BDEs and RSEs that are in good agreement with one another. Of the simpler methods, RBMK and RMPWB1K achieve good accuracy for BDEs and RSEs for all the species that were examined. For monosubstituted carbon-centered radicals, we find that the stabilizing effect (as measured by RSEs) of carbonyl substituents (CX═O) ranges from 24.7 to 36.9 kJ mol^{-1}, with the largest stabilization occurring for the CH═O group. Amino groups (NHY) also stabilize a monosubstituted α-carbon radical, with the calculated RSEs ranging from 44.5 to 49.5 kJ mol^{-1}, the largest stabilization occurring for the NH_2 group. In combination, NHY and CX═O substituents on a disubstituted carbon-centered radical produce a large stabilizing effect ranging from 82.0 to 125.8 kJ mol^{-1}. This translates to a captodative (synergistic) stabilization of 12.8 to 39.4 kJ mol^{-1}. For monosubstituted nitrogen-centered radicals, we find that the stabilizing effect of methyl and related (CH_2Z) substituents ranges from 25.9 to 31.7 kJ mol^{-1}, the largest stabilization occurring for the CH_3 group. Carbonyl substituents (CX═O) destabilize a nitrogen-centered radical relative to the corresponding closed-shell molecule, with the calculated RSEs ranging from −30.8 to −22.3 kJ mol^{-1}, the largest destabilization occurring for the CH═O group. In combination, CH_2Z and CX═O substituents at a nitrogen radical center produce a destabilizing effect ranging from −19.0 to −0.2 kJ mol^{-1}. This translates to an additional destabilization associated with disubstitution of −18.6 to −7.8 kJ mol^{-1}.

1. Introduction

Peptide radicals have been implicated in a number of diseases such as Alzheimer's disease, atherosclerosis, and diabetes as well as aging.[1−3] Studies of radicals on peptide backbones have revealed a special stability for α-carbon radicals. This has been attributed to the synergistic stabilization gained through the combined effect of the carbonyl and amide functionalities at the radical center,[1,4] which has been termed the captodative effect.[5]

In valence bond theory, the origin of the captodative effect can be explained in terms of a greater number of resonance-hybrid contributors in the disubstituted radical. For example, the resonance contributor IV in the glycyl radical:

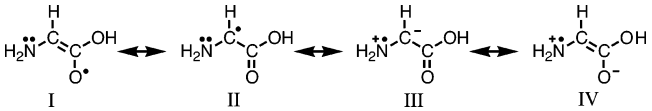

I II III IV

does not have a counterpart in the resonance contributors for the corresponding monosubstituted radicals, the carboxymethyl radical, and the aminomethyl radical:

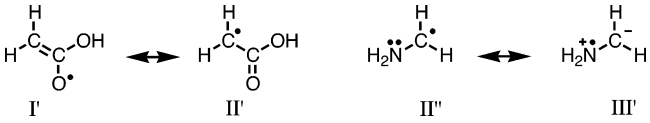

I' II' II" III'

In terms of molecular orbital theory, the appropriate orbital interactions are given in Figure 1. Figure 1a shows the interaction of the lone-pair orbital on the nitrogen of $NH_2-{}^{\bullet}CH_2$ with the singly occupied 2p(C$^{\bullet}$) orbital on carbon, lowering the energy of the lone-pair orbital and raising the energy of the 2p(C$^{\bullet}$) orbital, resulting in a net stabilization. Figure 1b shows that the raised 2p(C$^{\bullet}$) orbital interacts more effectively with the π^* orbital on the carbonyl, giving an increased stabilization.

A convenient measure of the effect of a substituent on the stability of a radical relative to its effect in the parent closed-shell molecule is given by the radical stabilization energy or RSE. For carbon-centered radicals the reference species is usually taken to be methane, while for nitrogen-centered radicals ammonia is normally used. The RSEs are defined by the energy changes in reactions 1 and 2:

$$^{\bullet}CH_2X + CH_4 \rightarrow CH_3X + {}^{\bullet}CH_3 \quad (1)$$

$$^{\bullet}NHX + NH_3 \rightarrow NH_2X + {}^{\bullet}NH_2 \quad (2)$$

Equivalently, the RSEs are equal to the difference between the bond dissociation energy (BDE) of the reference species and

* Address correspondence to this author. E-mail: radom@chem.usyd.edu.au.
† University of Sydney.
‡ Australian National University.
§ Present address: Department of Applied Chemistry, RMIT University, Melbourne, VIC 3000, Australia.

10.1021/jp051860a CCC: $30.25
Published on Web 06/23/2005

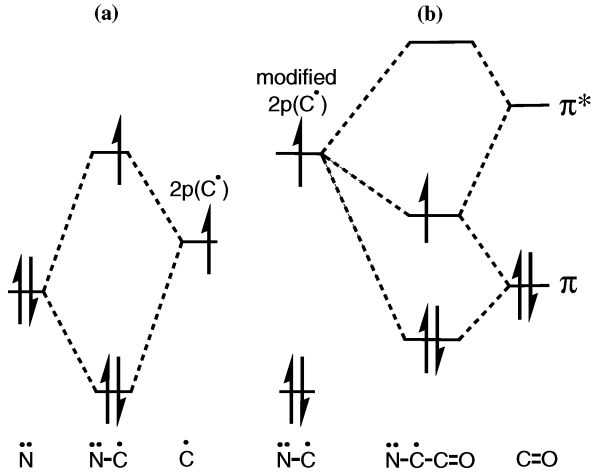

Figure 1. Orbital interaction diagram showing (a) the interaction of the singly occupied 2p orbital on the carbon, 2p(C•), with the lone pair on the nitrogen in $NH_2-{}^{\bullet}CH_2$, and (b**)** the enhanced interaction of the modified 2p(C•) orbital with the π^* orbital on the carbonyl group in $NH_2-{}^{\bullet}CH-CHO$.

the bond dissociation energy of the substituted species:

$$\mathrm{RSE}({}^{\bullet}\mathrm{CH_2X}) = \mathrm{BDE}(\mathrm{CH_4}) - \mathrm{BDE}(\mathrm{CH_3X}) \quad (3)$$

$$\mathrm{RSE}({}^{\bullet}\mathrm{NHX}) = \mathrm{BDE}(\mathrm{NH_3}) - \mathrm{BDE}(\mathrm{NH_2X}) \quad (4)$$

Defined in this way, a positive number implies a net stabilization of the substituted radical with respect to the reference radical relative to the same effect in the parent closed-shell species, while a negative number implies a net destablization.

Although the term RSE implies a measure of radical stability, it should be kept in mind that this is calculated relative to the parent species. Caution should be exercised when comparing RSEs of different systems where the closed-shell parents could themselves have a significant influence on the calculated RSE. This has been pointed out by Leroy and co-workers,[6] and also more recently by Coote et al.[7]

The deviation from additivity in the RSE of a disubstituted carbon-centered radical is given by:

$$\Delta(\mathrm{RSE}) = \mathrm{RSE}(\mathrm{X}-{}^{\bullet}\mathrm{CH}-\mathrm{Y}) - \mathrm{RSE}(\mathrm{X}-{}^{\bullet}\mathrm{CH}-\mathrm{H}) - \mathrm{RSE}(\mathrm{H}-{}^{\bullet}\mathrm{CH}-\mathrm{Y}) \quad (5)$$

Defined in this way, a positive Δ(RSE) means that the two substituents have a reinforcing stabilizing effect in the radical, a zero value would indicate that the RSEs are additive, and a negative number would indicate a destabilizing effect occurring in the disubstituted radical compared with the corresponding monosubstituted radicals (in all cases compared with the corresponding closed-shell molecules).

In a previous extensive study,[8] C−H BDEs leading to α-carbon radicals in a number of model systems containing a glycine peptide backbone were calculated with B3-LYP/6-31G(d). The calculated C−H BDEs for the model systems $HCONH_2-CH_2-CONH_2$, $CH_3CONH-CH_2-CONH_2$, $HCONH_2-CH_2-CONHCH_3$, and $CH_3CONH-CH_2-CONHCH_3$ were approximately equal, suggesting that an amide substituent on both sides of the α-carbon is sufficient to satisfactorily model the midchain environment of the C−H dissociation process. The accuracy of the BDEs calculated using B3-LYP/6-31G(d) were assessed against values obtained using the G2(MP2) high-level procedure.

In another recent study,[9] RSEs of α-carbon radicals were examined for the free amino acids, glycine, alanine, and valine, and their *N*-acetyl methyl esters. In that study, the ordering of RSEs for the *N*-acetyl methyl ester derivatives, which attempt to model a peptide environment, was found to differ from that for the free amino acids. For example, the largest RSE for the model peptides occurred for glycine, while the largest RSE for the free amino acids was found for alanine. The change in the ordering was attributed to steric interactions of the side-chain with the amide carbonyl groups. The RSEs of that study were evaluated with RMP2/6-31G(d)//UB3-LYP/6-31G(d). In another detailed study,[10] C−H BDEs were calculated for all the naturally occurring amino acids in model systems representative of a peptide backbone. It was found that the BDEs ranged from about 345 to 400 kJ mol^{-1}.

In the present study, we reexamine the C−H BDEs of model systems representing a glycine-containing peptide backbone using high-level procedures and a wider range of models. In addition, RSEs are calculated for the model peptides and compared with RSEs calculated for a series of monosubstituted analogues. In a similar manner, N−H BDEs and their associated RSEs are calculated for a similar series of model systems. The RSEs are used to examine the effect of substitution on a radical center and also to examine the deviation from additivity in the RSEs of the disubstituted systems.

2. Theoretical Methods

Standard ab initio molecular orbital theory and density functional theory (DFT) calculations were carried out with the Gaussian 03[11] and Molpro 2002.6[12] computer programs. Calculations on radicals that were performed with a restricted-open-shell reference wave function are designated with an "R" prefix (e.g., RMP2, RB3-LYP), while calculations using an unrestricted-open-shell wavefuction are designated with a "U" prefix (e.g., UMP2, UB3-LYP).

BDEs and RSEs were calculated with a number of theoretical procedures. First, a series of simpler methods were used. These involved both MP2 and DFT single-point calculations in association with the 6-311+G(3df,2p) basis set carried out on UB3-LYP/6-31G(d) optimized geometries. Energies were adjusted to 0 K by adding a scaled (by 0.9806[13]) UB3-LYP/6-31G(d) zero-point vibrational energy (ZPVE). The frozen-core (fc) approximation was employed in all MP2 calculations. DFT single-point calculations were carried out with the B3-LYP combination of exchange and correlation functionals and also with the recently formulated functionals BMK[14] and MPWB1K.[15] We found that the performance of these last two functionals is quite similar and so we only report on the BMK results throughout the text, but the results from the MPWB1K functional are available as Supporting Information.

In addition to the simpler methods, standard high-level procedures were used to calculate BDEs and RSEs. The G3X(MP2)-RAD[16] and CBS-QB3[17,18] procedures were used for all species, while a selection were also examined with the W1 method of Martin et al.[19] W1 is essentially based on the URCCSD(T) procedure of Molpro, extrapolated to the infinite-basis-set limit. For dissociations that lead to highly spin-contaminated radicals, it has been found recently that the calculated CBS-QB3 BDEs are often improved by omitting the empirical spin-correction term.[20,21] The resultant method has been termed U-CBS-QB3. A detailed study of the generality of this observation is in progress. In this connection, $\langle S^2 \rangle$ values quoted in the text are from MP2/6-311+G(3d2f,2df,2p)//B3-LYP/6-311G(2d,d,p) calculations, which is the method used to determine the CBS-QB3 spin-contamination correction term.

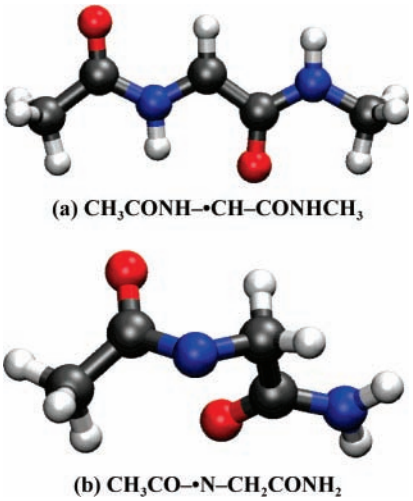

Figure 2. Optimized structures (B3-LYP/6-31G(d)) of the largest (a) carbon-centered radical ($CH_3CONH-{}^{\bullet}CH-CONHCH_3$) in an extended chain conformation and (b) the nitrogen-centered radical ($CH_3CO-{}^{\bullet}N-CH_2CONH_2$) demonstrating the puckering that occurs at the nitrogen carrying the unpaired electron.

B3-LYP/6-31G(d) optimized structures for each species can be obtained from Gaussian archive entries that are available as Supporting Information.

3. Results and Discussion

The conformational spaces for all species were initially scanned using UB3-LYP/6-31G(d). To aid the analysis, extended conformations (corresponding to Ramachandran angles close to 180°) were used whenever possible. Figure 2a shows the optimized structure of the largest carbon-centered radical examined in this study ($CH_3CONH-{}^{\bullet}CH-CONHCH_3$) in an extended chain conformation. In a small number of cases, the lowest-energy conformations correspond to folded structures due to internal hydrogen bonding. These were handled as described below.

For the species involved in the calculation of BDEs of carbon-centered radicals, the closed-shell molecule $CH_3CONH-CH_2-CONHCH_3$ is the only one in which the extended-chain conformation is not the global minimum.[22] The difference in energy between the global minimum and the extended-chain conformation in this case is approximately 3 kJ mol^{-1} at the CBS-QB3 level of theory. For the sake of consistency, the numbers quoted are those derived from the extended-chain conformation of this species, but this does not affect the qualitative trends in our analysis.

For the closed-shell counterparts of the nitrogen-centered radicals, the global minima all correspond to extended-chain conformations. For the nitrogen-centered radicals themselves, however, significant puckering occurs at the nitrogen carrying the unpaired electron. This makes it difficult in some cases to find conformations that do not contain some degree of internal hydrogen bonding. The species that are affected include the $CH_3CO-{}^{\bullet}NH-CH_2CHO$ and $CH_3CO-{}^{\bullet}NH-CH_2CONH_2$ radicals. Figure 2b shows the B3-LYP/6-31G(d) optimized structure of $CH_3CO-{}^{\bullet}NH-CH_2CONH_2$ that demonstrates the puckering that occurs on the nitrogen carrying the unpaired electron. The effect on the calculated BDEs and RSEs of the hydrogen bond that is present in these species is approximately 5 kJ mol^{-1}, based on constrained-optimized rotational potentials. It is not expected that our qualitative conclusions will be affected by including in the analysis conformers that involve some internal hydrogen bonding.

3.1. Bond Dissociation Energies. Bond dissociation energies (BDEs) for various molecules that represent systematically larger models of a peptide backbone containing a glycine residue are listed in Tables 1 (C−H BDEs) and 2 (N−H BDEs). We have chosen W1 as the benchmark theoretical method as it has been shown to give excellent agreement with reliable experimental thermochemistry.[23]

3.1.1. Carbon-Centered Radicals. W1 values for C−H BDEs have been calculated for four species, two of which have experimental values available for comparison. The calculated W1 BDEs at 0 K in these two cases, leading to the radicals $H-{}^{\bullet}CH-H$ and $H-{}^{\bullet}CH-CHO$, are 432.3 and 395.7 kJ mol^{-1}, respectively, compared with experimental values of 432.3 ± 0.4 and 389.5 ± 9.2 kJ mol^{-1}.

The computational expense of W1 prohibits the use of this procedure beyond moderately sized molecules. In a previous study of C−H BDEs,[24] the CBS-RAD procedure was found to provide a good secondary benchmark. In the present study, we have carried out calculations with CBS-QB3 in place of CBS-RAD, the two procedures having been found previously to give similar results.[25] We also report results obtained with the U-CBS-QB3 method because, as noted above, it has been found recently[20,21] that the calculated CBS-QB3 BDEs leading to highly spin-contaminated radicals are often improved by omitting the empirical spin-correction term. The radicals in Table 1 that have been calculated with W1 have $\langle S^2 \rangle$ values of 0.7616 ($H-{}^{\bullet}CH-H$), 0.9221 ($H-{}^{\bullet}CH-CHO$), 0.7626 ($NH_2-{}^{\bullet}CH-H$), and 0.8462 ($NH_2-{}^{\bullet}CH-CHO$). In the two cases that have large spin contamination, i.e., $H-{}^{\bullet}CH-CHO$ and $NH_2-{}^{\bullet}CH-CHO$, the calculated U-CBS-QB3 C−H BDEs are in closer agreement with the W1 values than are the standard CBS-QB3 values. Thus, for the purposes of this study we will use the U-CBS-QB3 BDEs as a secondary benchmark.

The largest spin-correction contribution to the CBS-QB3 procedure for the C−H BDEs examined in the present study amounts to −4.3 kJ mol^{-1} and occurs for $H-{}^{\bullet}CH-CHO$, which is the most highly spin-contaminated radical ($\langle S^2 \rangle = 0.9221$). There is a relatively small mean absolute deviation (MAD) of 1.3 kJ mol^{-1} between the standard CBS-QB3 BDEs and the U-CBS-QB3 BDEs. The MAD and the mean deviation (MD) for CBS-QB3 are the same magnitude because the spin-correction term is always negative.

The other high-level composite method in Table 1 is G3X(MP2)-RAD. The MAD from the BDEs calculated with U-CBS-QB3 is 2.5 kJ mol^{-1}, which demonstrates the good overall performance for this method. Unfortunately, as pointed out previously,[24] the largest deviation for this method (−5.4 kJ mol^{-1}) turns out to occur for the BDE of methane which, as will be seen, causes the radical stabilization energies (RSEs) to consistently be slightly underestimated.

In a previous study,[24] it was found that RB3-LYP/6-311+G(3df,2p)//RB3-LYP/6-31G(d) yielded good C−H BDEs. In that study, only monosubstituted species were considered. In the present study, RB3-LYP/6-311+G(3df,2p) single-point calculations on UB3-LYP/6-31G(d) optimized geometries lead to an MAD of 15.2 kJ mol^{-1}. The poorer overall performance of RB3-LYP in the present study arises because of the poorer results for the disubstituted radicals. Thus the *smallest* absolute deviation in the case of disubstuted radicals is 19.2 kJ mol^{-1} while the *largest* absolute deviation in the monosubstituted radicals is 14.1 kJ mol^{-1}. Using an unrestricted reference wave function instead of a restricted open-shell reference further increases the MAD, a trend also pointed out in the previous study.[24]

TABLE 1: Comparison of Calculated C−H Bond Dissociation Energies (0 K, kJ mol^{-1}) Resulting in the Formation of α-Carbon-Centered Radicals on Small Models of a Glycine-Containing Peptide Backbone

radical	UB3-LYP //B3[a]	RB3-LYP //B3[a]	UBMK //B3[a]	RBMK //B3[a]	RMP2 //B3[a]	G3X(MP2)-RAD	CBS-QB3	U-CBS-QB3[b]	W1
H−•CH−H	424.7	428.8	431.0	435.1	417.3	429.1	434.3	434.5	432.3
H−•CH−CHO	379.4	387.3	390.1	399.5	385.1	393.7	393.3	397.6	395.7
H−•CH−$CONH_2$	394.9	399.8	406.3	411.5	397.0	407.4	408.7	409.8	
H−•CH−$CONHCH_3$	393.8	398.4	404.5	409.4	396.8	407.1	408.6	409.4	
NH_2−•CH−H	369.4	373.3	376.3	380.2	371.5	384.2	384.7	385.0	383.1
HCONH−•CH−H	371.4	375.9	379.4	384.2	376.1	387.4	389.4	390.0	
CH_3CONH−•CH−H	371.1	375.3	379.3	383.8	375.3	386.8	389.0	389.4	
NH_2−•CH−CHO	282.2	286.5	292.5	297.9	291.1	312.3	306.3	308.7	309.3
NH_2−•CH−$CONH_2$	313.7	317.2	319.8	323.5	327.0	339.1	336.9	337.5	
HCONH−•CH−CHO	304.5	309.2	321.4	327.2	314.8	335.4	332.2	335.3	
HCONH −•CH−$CONH_2$	330.8	334.5	338.8	342.9	341.3	353.5	351.7	352.5	
CH_3CONH−•CH−$CONHCH_3$	328.3	331.8	337.7	341.5	339.6	347.6	350.5	351.0	
MAD[c]	19.7	15.2	10.3	6.0	14.0	2.5	1.3		
MD[c]	−19.7	−15.2	−10.3	−5.3	−14.0	−1.4	−1.3		
LD[c]	−30.8	−26.1	−17.8	−14.0	−20.5	−5.4	−4.3		

[a] Calculations have been performed in association with the 6-311+G(3df,2p) basis set on UB3-LYP/6-31G(d) optimized geometries. Energies have been corrected to 0 K using UB3-LYP/6-31G(d) ZPVEs scaled by 0.9806.[13] [b] Standard CBS-QB3 but with the empirical spin-correction for spin contamination in the unrestricted wave function omitted. [c] Mean absolute deviation (MAD), mean deviation (MD), and largest deviation (LD) from the calculated U-CBS-QB3 results.

TABLE 2: Comparison of Calculated N−H Bond Dissociation Energies (0 K, kJ mol^{-1}) Resulting in the Formation of Nitrogen-Centered Radicals on Small Models of a Glycine-Containing Peptide Backbone

radical	UB3-LYP //B3[a]	RB3-LYP //B3[a]	UBMK //B3[a]	RBMK //B3[a]	RMP2 //B3[a]	G3X(MP2)-RAD	CBS-QB3	U-CBS-QB3[b]	W1
H−•N−H	432.6	443.2	438.9	443.1	437.6	439.8	444.2	444.4	444.2
HCO−•N−H	461.6	471.6	473.0	483.7	481.1	469.3	470.2	475.2	474.3
CH_3CO−•N−H	449.8	458.3	463.4	472.4	473.0	462.4	463.2	466.7	
NH_2CH_2CO−•N−H	449.4	456.8	469.2	471.5	465.7	462.9	465.1	467.8	
H−•N−CH_3	395.9	401.0	403.2	407.8	408.2	409.4	412.4	412.7	412.2
H−•N−CH_2CHO	401.7	406.5	409.2	413.9	414.2	415.5	418.2	418.5	
H−•N−CH_2CONH_2	397.8	402.5	405.8	410.5	411.0	412.3	415.5	415.8	
HCO−•N−CH_3	434.9	441.6	445.4	453.0	456.0	447.8	447.7	451.3	
CH_3CO−•N−CH_3	426.1	431.9	438.3	444.2	448.2	441.4	442.4	444.6	
HCO−•N−CH_2CHO	461.6	454.0	458.9	465.5	465.9	458.8	461.1	463.4	
CH_3CO−•N−CH_2CHO	438.8	445.4	449.2	454.9	455.6	450.2	455.4	456.4	
CH_3CO−•N−CH_2CONH_2	440.6	446.4	452.1	457.1	456.6	451.3	455.7	456.7	
MAD[c]	15.2	9.5	5.8	3.3	3.9	4.4	1.9		
MD[c]	−15.2	−9.5	−5.6	+0.3	0.0	−4.4	−1.9		
LD[c]	−18.5	−13.3	−10.0	+8.5	−6.8	−6.2	−5.0		

[a] Calculations have been performed in association with the 6-311+G(3df,2p) basis set on UB3-LYP/6-31G(d) optimized geometries, energies have been corrected to 0 K using UB3-LYP/6-31G(d) ZPVEs scaled by 0.9806.[13] [b] Standard CBS-QB3 but with the empirical spin-correction for spin contamination in the unrestricted wave function omitted. [c] Mean absolute deviation (MAD), mean deviation (MD), and largest deviation (LD) from the calculated U-CBS-QB3 results.

RMP2/6-311+G(3df,2p)//UB3-LYP/6-31G(d) produces an MAD of 14.0 kJ mol^{-1}. This is a small improvement over RB3-LYP. For this method, the deviations from the U-CBS-QB3 values are equally large for the disubstituted radicals and the monosubstituted radicals.

Single-point calculations with the recently formulated BMK functional of Boese and Martin[14] give good results for C−H BDEs. For UBMK, the MAD is 10.3 kJ mol^{-1}, while RBMK gives an MAD of 6.0 kJ mol^{-1}. Considering the modest cost of this method, these results are very encouraging. As with RB3-LYP, larger absolute deviations occur for disubstituted systems compared with monosubstituted systems. It should be noted that this does not necessarily represent a correlation in the error with the size of the molecules involved since some of the disubstituted systems are smaller than the monosubstituted species.

3.1.2. Nitrogen-Centered Radicals. Listed in Table 2 are N−H BDEs that lead to nitrogen-centered radicals on small models of a peptide backbone containing a glycine residue. U-CBS-QB3 has been found previously to give better agreement with W1 than standard CBS-QB3 for N−H BDEs.[20] Therefore, we again use U-CBS-QB3 values as a secondary benchmark and compare values obtained with other methods with the U-CBS-QB3 results.

Standard CBS-QB3 shows only a small deviation from the U-CBS-QB3 values, with an MAD of 1.9 kJ mol^{-1}. The largest deviation occurs for the HCO−•N−H radical, which has an $\langle S^2 \rangle$ value of 0.9482.

The BDEs found with the high-level G3X(MP2)-RAD procedure also compare well with the BDEs found with U-CBS-QB3 for nitrogen-centered radicals. The MAD is 4.4 kJ mol^{-1}.

In a previous study,[20] it was found that RMP2 did not perform as well for the calculation of N−H BDEs as it did for C−H BDEs. This does not appear to be the case in the present study. The MAD for the RMP2 N−H BDEs is 3.9 kJ mol^{-1}, which is a more satisfactory result than for the current C−H BDEs.

As with the C−H BDEs, the DFT methods that are examined in Table 2 are improved by using a restricted reference wave function instead of an unrestricted reference wave function. For example, the MAD for the N−H BDEs obtained with UB3-LYP is 15.2 kJ mol^{-1} compared with the RB3-LYP value of 9.5 kJ mol^{-1}. The BMK results are also affected in the same

TABLE 3: Comparison of Calculated Radical Stabilization Energies (0 K, kJ mol^{-1}) of α-Carbon Radicals on Small Models of a Glycine-Containing Peptide Backbone

radical	UB3-LYP //B3[a]	RB3-LYP //B3[a]	UBMK //B3[a]	RBMK //B3[a]	RMP2 //B3[a]	G3X(MP2)-RAD	CBS-QB3	U-CBS-QB3[b]	W1
H−•CH−CHO	45.3	41.5	43.6	40.9	32.2	35.4	41.0	36.9	36.6
H−•CH−$CONH_2$	29.8	29.0	27.0	25.5	20.3	21.7	25.6	24.7	
H−•CH−$CONHCH_3$	30.9	30.4	27.7	26.7	20.5	22.0	25.7	25.1	
NH_2−•CH−H	55.3	55.5	55.1	54.7	45.8	44.9	49.6	49.5	49.2
HCONH−•CH−H	53.3	53.0	50.2	49.1	41.2	41.7	44.9	44.5	
CH_3CONH−•CH−H	53.6	53.5	50.7	49.9	42.0	42.3	45.3	45.1	
NH_2−•CH−CHO	142.5	142.3	140.1	137.2	126.2	116.8	128.0	125.8	123.0
NH_2−•CH−$CONH_2$	111.0	111.6	107.8	107.4	90.3	90.0	97.4	97.0	
HCONH−•CH−CHO	120.2	119.7	116.3	112.9	102.5	93.7	102.1	99.2	
HCONH−•CH−$CONH_2$	93.9	94.4	89.3	88.6	76.0	75.6	82.6	82.0	
CH_3CONH−•CH−$CONHCH_3$	96.4	97.0	91.9	91.5	77.7	81.5	83.8	83.5	
MAD[c]	10.8	10.4	7.4	6.5	4.2	4.3	1.2		
MD[c]	+10.8	+10.4	+7.4	+6.9	−3.5	−4.3	+1.2		
LD[c]	+21.0	+20.5	+14.2	+14.6	−6.7	−9.0	+4.1		

[a] Calculations have been performed in association with the 6-311+G(3df,2p) basis set on UB3-LYP/6-31G(d) optimized geometries. Energies have been corrected to 0 K using UB3-LYP/6-31G(d) ZPVEs scaled by 0.9806.[13] [b] Standard CBS-QB3 but with the empirical spin-correction for spin contamination in the unrestricted wave function omitted. [c] Mean absolute deviation (MAD), mean deviation (MD), and largest deviation (LD) from the calculated U-CBS-QB3 results.

TABLE 4: Comparison of Calculated Radical Stabilization Energies (0 K, kJ mol^{-1}) of Nitrogen-Centered Radicals on Small Models of a Glycine-Containing Peptide Backbone

radical	UB3-LYP //B3[a]	RB3-LYP //B3[a]	UBMK //B3[a]	RBMK //B3[a]	RMP2 //B3[a]	G3X(MP2)-RAD	CBS-QB3	U-CBS-QB3[b]	W1
HCO−•N−H	−29.0	−28.4	−34.1	−40.6	−43.5	−29.5	−26.0	−30.8	−30.1
CH_3CO−•N−H	−17.2	−15.1	−24.5	−29.3	−35.4	−22.6	−19.0	−22.3	
NH_2CH_2CO−•N−H	−16.8	−13.6	−30.3	−28.4	−28.1	−23.1	−20.9	−23.4	
H−•N−CH_3	36.7	42.2	35.7	35.3	29.4	30.4	31.8	31.7	32.0
H−•N−CH_2CHO	30.9	36.7	29.7	29.2	23.4	24.3	26.0	25.9	
H−•N−CH_2CONH_2	34.8	40.7	33.1	32.6	26.6	27.5	28.7	28.6	
HCO−•N−CH_3	−2.3	1.6	−6.5	−9.9	−18.4	−8.0	−3.5	−6.9	
CH_3CO−•N−CH_3	6.5	11.3	0.6	−1.1	−10.6	−1.6	1.8	−0.2	
HCO−•N−CH_2CHO	−29.0	−10.8	−20.0	−22.4	−28.3	−19.0	−16.9	−19.0	
CH_3CO−•N−CH_2CHO	−6.2	−2.2	−10.3	−11.8	−18.0	−10.4	−11.2	−12.0	
CH_3CO−•N−CH_2CONH_2	−8.0	−3.2	−13.2	−14.0	−19.0	−11.5	−11.5	−12.3	
MAD[c]	5.5	9.1	2.7	3.8	7.4	1.0	1.8		
MD[c]	+3.7	+9.1	+0.1	−1.8	−7.4	−0.3	+1.8		
LD[c]	−10.6	+12.1	−6.9	−9.8	−13.1	−1.6	+4.8		

[a] Calculations have been performed in association with the 6-311+G(3df,2p) basis set on UB3-LYP/6-31G(d) optimized geometries. Energies have been corrected to 0 K using UB3-LYP/6-31G(d) ZPVEs scaled by 0.9806.[13] [b] Standard CBS-QB3 but with the empirical spin-correction for spin contamination in the unrestricted wave function omitted. [c] Mean absolute deviation (MAD), mean deviation (MD), and largest deviation (LD) from the calculated U-CBS-QB3 results.

way. The N−H BDEs calculated with UBMK have an MAD of 5.8 kJ mol^{-1}, compared with 3.3 kJ mol^{-1} for RBMK. The results found with RBMK for the N−H BDEs are very encouraging, as was also the case for C−H BDEs, especially when considering the modest computational cost of this method. In fact, the performance of RBMK for N−H BDEs is comparable to that of the high level G3X(MP2)-RAD procedure.

Apart from RBMK, the DFT methods examined in Table 2 generally underestimate N−H BDEs. This is reflected in the MDs and MADs having the same magnitude. We noted above that the C−H BDEs calculated with DFT procedures for disubstituted systems are not as good as those for monosubstituted radicals. In the case of the N−H BDEs, the larger absolute deviations from the benchmark values occur for species that are larger in size (rather than for disubstituted versus monosubstituted).

3.2. Radical Stabilization Energies. Tables 3 and 4 present radical stabilization energies (RSEs) for carbon- and nitrogen-centered radicals, respectively, associated with small models of a glycine-containing peptide backbone. Systematic errors in the calculation of BDEs can cancel in the evaluation of RSEs. This can mean that methods that perform less well in predicting BDEs may still produce acceptable RSEs.

3.2.1. Carbon-Centered Radicals. RSEs calculated with U-CBS-QB3 are taken as a secondary benchmark because of the enhanced agreement with W1. Most of the methods displayed in Table 3 perform better in determining RSEs than BDEs, as shown by the smaller MADs and MDs in this table compared with the MADs and MDs in Table 1. Standard CBS-QB3 compares well with U-CBS-QB3, with an MAD of 1.2 kJ mol^{-1}.

The G3X(MP2)-RAD method is the only method to have a worse MAD for the RSEs than for the BDEs though, even in this case, the MAD for the RSEs is an acceptable 4.3 kJ mol^{-1}. The origin of the problem in calculating RSEs with G3X(MP2)-RAD lies with the greater-than-expected deviation of this method for the BDE of methane, leading to the observed underestimation of the RSEs. The RMP2 RSEs of Table 3 also are quite acceptable, with an MAD of 4.2 kJ mol^{-1}.

Of the DFT methods, RBMK performs the best with an MAD of 6.9 kJ mol^{-1}. Using UBMK makes the agreement less good for the RSEs (MAD = 7.4 kJ mol^{-1}) but the effect is not as

pronounced as for the BDEs where the MAD is almost doubled. Both RBMK and UBMK systematically overestimate the RSEs, resulting in MADs and MDs that are the same in magnitude. These effects are also seen with RB3-LYP and UB3-LYP where the MADs are 10.4 and 10.8 kJ mol^{-1}, respectively.

The U-CBS-QB3 results in Table 3 show that the carbonyl-substituted radicals have RSEs between 24.7 and 36.9 kJ mol^{-1}. The origin of the stabilization of a carbon radical center by a CX═O group has been explained in detail elsewhere.[24] Briefly, the π and π* orbitals on the carbonyl can interact with the singly occupied 2p carbon orbital, 2p(C•), producing a net stabilization. The smaller the energy separation between the 2p(C•) orbital on the carbon and the π* orbital on the carbonyl, the greater the stabilizing effect.

The formyl group (CH═O) has a greater stabilizing effect on the radical than a formamidyl group (C═ONH$_2$), as reflected in the U-CBS-QB3 RSEs of 36.9 and 24.7 kJ mol^{-1} for H−•CH−CHO and H−•CH−CONH$_2$, respectively. This arises because the NH$_2$ substituent decreases the π-accepting ability of the CH═O group. Further replacement of an amino hydrogen on the formamidyl group with a methyl group, to give the H−•CH−CONHCH$_3$ radical, has only a minor further effect on stabilization, evident in the small change in the RSE calculated with U-CBS-QB3 from 24.7 to 25.1 kJ mol^{-1} for H−•CH−CONH$_2$ and H−•CH−CONHCH$_3$, respectively. This suggests that the stability of a monosubstituted α-carbon radical will not generally be significantly affected by substituents beyond the amide bond, and supports previous conclusions to this effect.[8]

Amine (NHY) functionalities also stabilize carbon-centered radicals. The calculated U-CBS-QB3 RSE for aminomethyl radical (NH$_2$−•CH−H) is 49.5 kJ mol^{-1}. The large stabilizing effect arises from the interaction of the nitrogen lone-pair orbital with the 2p(C•) orbital on the carbon, as shown in Figure 1a.

Formally replacing an amino hydrogen with a formyl group results in the HCONH−•CH−H radical. The calculated U-CBS-QB3 RSE for this radical is 44.5 kJ mol^{-1}. This amounts to a change in the RSE of 5.0 kJ mol^{-1} in going from NH$_2$−•CH−H to CHONH−•CH−H, resulting from a decreased π-electron-donating ability of CHONH compared with NH$_2$. This change is relatively minor compared with the change in the RSE of the carbonyl-substituted radicals, H−•CH−CHO and H−•CH−CONH$_2$, of 12.2 kJ mol^{-1}. Thus, formation of an amide bond affects the π-donating ability of the nitrogen lone pair in this environment significantly less than the π-accepting ability of the carbonyl. Although there are many factors involved in the stabilization of each radical, calculated spin densities at the radical center are consistent with this result. The UB3-LYP/6-31G(d) spin densities on the carbon formally carrying the unpaired electron are +0.903 (NH$_2$−•CH−H), +0.904 (CHONH−•CH−H), +0.864 (H−•CH−CHO), and +0.983 (H−•CH−CONH$_2$). These results show that there is only a small change in spin density accompanying formyl substitution in NH$_2$−•CH−H, but there is a larger positive change accompanying amino substitution in H−•CH−CHO.

An additional methyl substituent, giving the CH$_3$CONH−•CH−H radical, results in a calculated U-CBS-QB3 RSE of 45.1 kJ mol^{-1}, a change of just 0.6 kJ mol^{-1} from the RSE of CHONH−•CH−H. As with the situation for the carbonyl-substituted radicals, substitution beyond the initial amide bond has little effect on the RSE for monosubstituted α-carbon radicals, again supporting previous conclusions.[8]

The calculated U-CBS-QB3 RSEs for the disubstituted carbon-centered radicals range between 82.0 and 125.8 kJ mol^{-1}, indicating much larger stabilizing effects than observed in the monosubstituted radicals (Table 5). The simplest disubstituted radical (NH$_2$−•CH−CHO) has a calculated U-CBS-QB3 RSE of 125.8 kJ mol^{-1}, which is the largest value in the table. The deviation from additivity evaluated with eq 5, given in the final column of Table 5, is 39.4 kJ mol^{-1}. For the monosubstituted radicals a change from H−•CH−CHO to H−•CH−CONH$_2$ decreases the RSE by 15.3 kJ mol^{-1}. For the equivalent change in the disubstituted radicals, resulting in NH$_2$−•CH−CONH$_2$, the RSE decreases by 28.8 kJ mol^{-1}. This indicates that not only is there a decrease in stability arising from the poorer π-accepting ability of the C═ONH$_2$ group but there is also a decrease in the synergistic interaction, as demonstrated by the reduced deviation from additivity from 39.4 to 15.7 kJ mol^{-1}.

TABLE 5: Comparison of Radical Stabilization Energies of Carbon-Centered Radicals (0 K, kJ mol^{-1}) Calculated with U-CBS-QB3[a] for Disubstituted Radicals (X−•CH−Y) with Values for the Corresponding Monosubstituted Radicals (X−•CH−H and H−•CH−Y)

X−•CH−Y	X−•CH−H	H−•CH−Y	X−•CH−Y	Δ(RSE)[b]
NH$_2$−•CH−CHO	49.5	36.9	125.8	39.4
NH$_2$−•CH−CONH$_2$	49.5	24.7	97.0	15.7
HCONH−•CH−CHO	44.5	36.9	99.2	17.8
HCONH−•CH−CONH$_2$	44.5	24.7	82.0	12.8
CH$_3$CONH−•CH−CONHCH$_3$	45.1	25.1	83.5	13.3

[a] Standard CBS-QB3 but with the empirical spin-correction for spin-contamination in the unrestricted wave function omitted. [b] The estimated synergistic stabilization (captodative effect) of two groups working in combination, measured by taking the difference between the RSE calculated for the disubstituted radical and the sum of the RSEs calculated for the analogous monosubstituted radicals, i.e., RSE(X−•CH−Y) − RSE(X−•CH−H) − RSE(H−•CH−Y).

Formyl substitution in NH$_2$−•CH−CHO leads to CHONH−•CH−CHO, which has a U-CBS-QB3 RSE of 99.2 kJ mol^{-1}. This represents a decrease of 26.6 kJ mol^{-1}. The deviation from additivity in this case is 17.8 kJ mol^{-1}. Thus, the decreased π-donating ability of the nitrogen lone-pair associated with formyl substitution also causes the loss of approximately half the synergistic stabilization.

Further losses in synergistic stabilization for radicals derived from molecules beyond the first amide bond are small, as reflected in the Δ(RSE) for HCONH−•CH−CONH$_2$ (12.8 kJ mol^{-1}) and CH$_3$CONH−•CH−CONHCH$_3$ (13.3 kJ mol^{-1}).

3.2.2. Nitrogen-Centered Radicals. The RSEs for nitrogen-centered radicals in a model peptide backbone are presented in Table 4.

The standard CBS-QB3 RSEs compare well with the values calculated with U-CBS-QB3, with an MAD of just 1.8 kJ mol^{-1}. This is expected because of the small size of the empirical spin-correction term.

The RSEs calculated with G3X(MP2)-RAD are also in good agreement with the RSEs calculated with U-CBS-QB3, with an MAD of 1.0 kJ mol^{-1}. In the case of nitrogen-centered radicals, the RSEs do not suffer the problem encountered with the RSEs of carbon-centered radicals, i.e., there is a smaller error in the calculated BDE of ammonia compared with the error in the calculated BDE of methane.

RMP2 performs reasonably well for the calculation of RSEs of nitrogen-centered radicals, with an MAD of 7.4 kJ mol^{-1}.

The DFT methods also perform reasonably well. However, the previously observed trend in which the restricted reference wave function improves the calculated BDEs compared with those obtained with an unrestricted reference wave function is reversed. For example, the MAD for RB3-LYP is 9.1 kJ mol^{-1},

TABLE 6: Comparison of Radical Stabilization Energies of Nitrogen-Centered Radicals (0 K, kJ mol^{-1}) Calculated with U-CBS-QB3[a] for Disubstituted Radicals (X−•CH−Y) with Values for the Corresponding Monosubstituted Radicals (X−•CH−H and H−•CH−Y)

X−•N−Y	X−•N−H	H−•N−Y	X−•N−Y	Δ(RSE)[b]
HCO−•N−CH_3	−30.8	31.7	−6.9	−7.8
CH_3CO−•N−CH_3	−22.3	31.7	−0.2	−9.6
HCO−•N−CH_2CHO	−30.8	25.9	−19.0	−14.1
CH_3CO−•N−CH_2CHO	−22.3	25.9	−12.0	−15.6
CH_3CO−•N−CH_2CONH_2	−22.3	28.6	−12.3	−18.6

[a] Standard CBS-QB3 but with the empirical spin-correction for spin-contamination in the unrestricted wave function omitted. [b] The calculated deviation from additivity of two groups working in combination, measured by taking the difference of the RSE calculated for the disubstituted radical with the sum of the RSEs calculated for the analogous monosubstituted radicals, i.e., RSE(X−•CH−Y) − RSE(X−•CH−H) − RSE(H−•CH−Y).

compared with 5.5 kJ mol^{-1} for UB3-LYP. The trend is the same for the BMK functional, with MADs of 3.8 (RBMK) and 2.7 (UBMK) kJ mol^{-1}.

Table 6 compares RSEs calculated with the U-CBS-QB3 procedure for disubstituted nitrogen-centered radicals and their monosubstituted analogues. The monosubstituted radicals of this table can be grouped according to whether a CX═O group or a CH_2Z group is attached to the radical center. For the CH_2Z substituents, the RSEs range between 25.9 and 31.7 kJ mol^{-1}, indicating that they are stabilizing substituents. On the other hand, the RSEs for the carbonyl (CX═O) substituents range between −22.3 and −30.8 kJ mol^{-1} representing a destabilizing effect for this substituent compared with their effect in the closed-shell parents. The reason for the stabilization in the case of the methyl group and the destabilization in the case of the carbonyl group has been explained in detail elsewhere.[20,26] Briefly, stabilization of the radical by CH_2Z can occur through a hyperconjugative interaction, which is not present to the same extent in the parent closed-shell species. For the carbonyl substituents, the observed destabilization occurs because in the closed-shell parent species it is the nitrogen lone pair that is delocalized, whereas in the radical, it is the single unpaired electron that interacts with the π^* orbital. In both cases, the stabilizing or destabilizing effect of the substituent is attenuated as the chain becomes longer.

For disubstituted nitrogen-centered radicals, the RSEs range between −19.0 and −0.2 kJ mol^{-1}, indicating a net destabilization in all cases. This contrasts with the behavior of the carbon-centered radicals, which benefit through a captodative stabilization from disubstitution. For example, the RSE of H−•N−CH_3 is calculated to be 31.7 kJ mol^{-1} and the calculated RSE of HCO−•N−H is −30.8 kJ mol^{-1}, whereas the calculated RSE of HCO−•N−CH_3 is −6.9 kJ mol^{-1}. If the effect of the two substituents were exactly additive, then the RSE of HCO−•N−CH_3 would be 0.9 kJ mol^{-1}. Similar behavior is seen for the larger nitrogen-centered radicals where the Δ(RSE) values range from −18.6 to −9.6 kJ mol^{-1}. These negative values could arise either from additional destabilization in the N-centered radicals or as a result of additional stabilization in the disubstituted closed-shell parent species. To distinguish between these two possibilities, we have calculated the enthalpies of reactions 6 and 7:

$$X{-}NH{-}Y + NH_3 \rightarrow X{-}NH_2 + Y{-}NH_2 \quad (6)$$

$$X{-}N^{\bullet}{-}Y + {}^{\bullet}NH_2 \rightarrow X{-}{}^{\bullet}NH + Y{-}{}^{\bullet}NH \quad (7)$$

TABLE 7: Comparison of Enthalpies of Reactions Measuring Stabilizing Interactions at N and N• (U-CBS-QB3,[a] 0 K, kJ mol^{-1})

X−(N)−Y[b]	X−NH−Y[c]	X−•N−Y[d]	$\Delta\Delta H$[e]
HCO−(N)-CH_3	25.5	17.6	−7.8
CH_3CO−(N)-CH_3	25.9	16.4	−9.6
HCO−(N)−CH_2CHO	25.3	11.2	−14.1
CH_3CO−(N)−CH_2CHO	28.2	12.7	−15.6
CH_3CO−(N)−CH_2CONH_2	31.2	12.5	−18.6

[a] Standard CBS-QB3 but with the empirical spin-correction for spin-contamination in the unrestricted wave function omitted. [b] (N) = NH or •N. [c] Enthalpy change for X−NH−Y + NH_3 → X−NH_2 + Y−NH_2. [d] Enthalpy change for X−•N−Y + •NH_2 → X−•NH + Y−•NH. [e] Equivalent to Δ(RSE).

These provide a measure of the respective stabilizing effects of disubstitution in the closed-shell parent species and the analogous N-centered radicals. We find (Table 7) that disubstitution has a greater stabilizing effect in the closed-shell parent species, and this in turn leads to the observed negative Δ(RSE) values.

4. Concluding Remarks

Bond dissociation energies (BDEs) and radical stabilization energies (RSEs) have been calculated for a series of molecules that represent the backbone of a small glycine-containing peptide. The resultant radicals are either carbon-centered, at the α-carbon, or nitrogen-centered, on the backbone nitrogens. We find both for BDEs and RSEs that the high-level theoretical procedures G3X(MP2)-RAD, CBS-QB3, and U-CBS-QB3 give results that are in good agreement with one another, and with W1 values in the few cases where the latter are available. U-CBS-QB3 performs slightly better than standard CBS-QB3 for spin-contaminated radicals, and we use this method as a secondary benchmark.

Of the less computationally demanding methods, RBMK/6-311+G(3df,2p), RMPWB1K/6-311+G(3df,2p), and RMP2/6-311+G(3df,2p), carried out with UB3-LYP/6−31(d) geometries, perform well for BDEs. For RSEs, the restricted and unrestricted forms of BMK/6-311+G(3df,2p)//UB3-LYP/6-31G(d) and MPWB1K/6-311+G(3df,2p)//UB3-LYP/6-31G(d) give results in very good agreement with the U-CBS-QB3 values. The MPWB1K results are available as Supporting Information.

Positive RSEs (indicating a relative stabilization) are found for monosubstituted carbon-centered radicals for both amine (NHY) and carbonyl (CX═O) substituents, with the NHY substituents being the more effective stabilizing groups. The disubstituted radicals are further stabilized through a large captodative interaction.

For monosubstituted nitrogen-centered radicals, we find positive RSEs for methyl and related (CH_2Z) substituents, while we find negative RSEs for the CX═O substituents. An effective additional destabilization occurs for the disubstituted radicals.

Acknowledgment. We gratefully acknowledge generous allocations of computer time from the ANU Supercomputing Facility, the Australian Partnership for Advanced Computing (APAC), and the Australian Centre for Advanced Computing and Communications (AC3), as well as the award of an Australian Research Council Discovery Grant (to L.R.), an Australian Postgraduate Award (to G.P.F.W.), and a University of Sydney Sesqui Research Fellowship (to D.M.).

Supporting Information Available: UB3-LYP/6-31G(d) GAUSSIAN archive entries of equilibrium structures are given

in Table S1, UMPWB1K and RMPWB1K BDEs in Table S2, and UMPWB1K and RMPWB1K RSEs in Table S3. This material is available free of charge via the Internet at http://pubs.acs.org.

References and Notes

(1) Davies, M. J.; Dean, R. T. *Radical-Mediated Protein Oxidation*: *from Chemistry to Medicine*; Oxford University Press: New York, 1997; and references therein.

(2) Dean, R. T.; Fu, S.; Stocker, R.; Davies, M. J. *Biochem. J.* **1997**, *324*, 1−18.

(3) (a) Brunelle, P.; Rauk, A. *J. Alzheimer's Dis.* **2002**, *4*, 283−289. (b) Rauk, A. *Can. Chem. News* **2001**, *53*, 20−21. (c) Rauk, A.; Armstrong, D. A.; Fairlie, D. P. *J. Am. Chem. Soc.* **2000**, *122*, 9761−9767.

(4) Easton, C. J. *Chem. Rev.* **1997**, *97*, 53−82 and references therein.

(5) Viehe, H. G.; Janousek, Z.; Merenyi, R.; Stella, L. *Acc. Chem. Res.*, **1985**, *18*, 148−154.

(6) Leroy, G.; Sana, M.; Wilante, C.; van Zieleghem, M.-J. *J. Mol. Struct.* (*THEOCHEM*) **1991**, *247*, 199−215.

(7) Coote, M. L.; Pross, A.; Radom, L. *Org. Lett.* **2003**, *5*, 4689−4692.

(8) Armstrong, D. A.; Yu, D.; Rauk, A. *Can. J. Chem.* **1996**, *74*, 1192−7207.

(9) Croft, A. K.; Easton, C. J.; Radom, L. *J. Am. Chem. Soc.* **2003**, *125*, 4119−4124.

(10) Rauk, A.; Yu, D.; Taylor, J.; Shustov, G. V.; Block, D. A.; Armstrong, D. A. *Biochemistry* **1999**, *38*, 9089−9096.

(11) Frisch, M. J.; Trucks, G. W.; Schlegel, H. B.; Scuseria, G. E.; Robb, M. A.; Cheeseman, J. R.; Montgomery, J. A., Jr.; Vreven, T.; Kudin, K. N.; Burant, J. C.; Millam, J. M.; Iyengar, S. S.; Tomasi, J.; Barone, V.; Mennucci, B.; Cossi, M.; Scalmani, G.; Rega, N.; Petersson, G. A.; Nakatsuji, H.; Hada, M.; Ehara, M.; Toyota, K.; Fukuda, R.; Hasegawa, J.; Ishida, M.; Nakajima, T.; Honda, Y.; Kitao, O.; Nakai, H.; Klene, M.; Li, X.; Knox, J. E.; Hratchian, H. P.; Cross, J. B.; Adamo, C.; Jaramillo, J.; Gomperts, R.; Stratmann, R. E.; Yazyev, O.; Austin, A. J.; Cammi, R.; Pomelli, C.; Ochterski, J. W.; Ayala, P. Y.; Morokuma, K.; Voth, G. A.; Salvador, P.; Dannenberg, J. J.; Zakrzewski, V. G.; Dapprich, S.; Daniels, A. D.; Strain, M. C.; Farkas, O.; Malick, D. K.; Rabuck, A. D.; Raghavachari, K.; Foresman, J. B.; Ortiz, J. V.; Cui, Q.; Baboul, A. G.; Clifford, S.; Cioslowski, J.; Stefanov, B. B.; Liu, G.; Liashenko, A.; Piskorz, P.; Komaromi, I.; Martin, R. L.; Fox, D. J.; Keith, T.; Al-Laham, M. A.; Peng, C. Y.; Nanayakkara, A.; Challacombe, M.; Gill, P. M. W.; Johnson, B.; Chen, W.; Wong, M. W.; Gonzalez, C.; Pople, J. A. *Gaussian 03*, Revision C.02; Gaussian, Inc.: Pittsburgh, PA, 2003.

(12) Werner, H.-J.; Knowles, P. J.; Amos, R. D.; Bernhardsson, A.; Berning, A.; Celani, P.; Cooper, D. L.; Deegan, M. J. O.; Dobbyn, A. J.; Eckert, F.; Hampel, C.; Hetzer, G.; Knowles, P. J.; Korona, T.; Lindh, R.; Lloyd, A. W.; McNicholas, S. J.; Manby, F. R.; Meyer, W.; Mura, M. E.; Nicklass, A.; Palmieri, P.; Pitzer, R.; Rauhut, G.; Schutz, M.; Schumann, U.; Stoll, H.; Stone, A. J.; Tarroni, R.; Thorsteinsson, T. *MOLPRO 2002.6*; University of Birmingham: Birmingham, U.K., 2002.

(13) Scott, A. P.; Radom, L. *J. Phys. Chem.* **1996**, *100*, 16502−16513.

(14) Boese, D. A.; Martin, J. M. L. *J. Chem. Phys.* **2004**, *121*, 3405−3416.

(15) Zhao, Y.; Truhlar, D. G. *J. Phys. Chem. A* **2004**, *108*, 6908−6918.

(16) Henry, D. J.; Sullivan, M. B.; Radom, L. *J. Chem. Phys.* **2003**, *118*, 4849−4860.

(17) Montgomery, J. A., Jr.; Frisch, M. J.; Ochterski, J. W.; Petersson, G. A. *J. Chem. Phys.* **1999**, *110*, 2822−2827. The CBS-QB3 procedure was employed instead of our previously used CBS-RAD method (see ref 18) because it includes re-optimization of the three CBS empirical parameters that are used in conjunction with B3-LYP optimized structures and frequencies.

(18) Mayer, P. M.; Parkinson, C. J.; Smith, D. M.; Radom, L. *J. Chem. Phys.* **1998**, *108*, 604−615.

(19) Martin, J. M. L.; De Oliveira, G. J. *J. Chem. Phys.* **1999**, *111*, 1843−1856.

(20) Wood, G. P. F.; Henry, D. J.; Radom, L. *J. Phys. Chem. A* **2003**, *107*, 7985−7990.

(21) Coote, M. L. *J. Phys. Chem. A* **2004**, *108*, 3865−3872.

(22) Figure S1 in the Supporting Information displays the global minimum and extended-chain conformations of this species.

(23) Parthiban, S.; Martin, J. M. L *J. Chem. Phys.* **2001**, *114*, 6014−6029.

(24) See, for example: Henry, D. J.; Parkinson, C. J.; Mayer, P. M.; Radom, L *J. Phys. Chem. A* **2001**, *105*, 6750−6756.

(25) Henry, D. J.; Parkinson, C. J.; Radom, L *J. Phys. Chem. A* **2002**, *106*, 7927−7936.

(26) Song, K. S.; Cheng, Y. H.; Fu, Y.; Liu, L.; Li, X. S.; Guo, Q. X. *J. Phys. Chem. A* **2002**, *106*, 6651−6658.